[4]T. R. Koehler, Phys. Rev. Letters 17, 89 (1966).
[5]P. Choquard, *The Anharmonic Crystal* (Benjamin, New York, 1967).
[6]H. Horner, Z. Physik 205, 72 (1967).
[7]T. R. Koehler, N. S. Gillis, and N. R. Werthamer, Phys. Rev. 165, 951 (1968).
[8]L. H. Nosanow, Phys. Rev. 146, 20 (1966).
[9]J. H. Hetherington, W. J. Mullin, and L. H. Nosanow, Phys. Rev. 154, 175 (1967).
[10]C. W. Woo and W. E. Massey, Phys. Rev. 169, 241 (1968).
[11]R. A. Guyer, Solid State Commun. 7, 315 (1969); in *Solid State Physics*, edited by F. Seitz, D. Turnbull, and H. Ehrenreich (Academic, New York, 1969), Vol. 23, p. 413; R. A. Guyer and L. I. Zane, Phys. Rev. 188, 445 (1969).
[12]B. Sarkissian, Ph. D. thesis (Duke University, 1969) (unpublished).
[13]When discussing the work of Guyer and Sarkissian, we will generally use the single reference 11. It should be pointed out, however, that many of the numerical results described in these articles were first calculated by Sarkissian in Ref. 12, which is less readily available.
[14]H. Horner, Phys. Rev. A 1, 1722 (1970).
[15]F. Iwamoto and H. Namaizawa, Progr. Theoret. Phys. (Kyoto) Suppl. 37/38, 234 (1966); and unpublished.
[16]K. A. Brueckner and J. Frohberg, Progr. Theoret. Phys. (Kyoto) Suppl. Ext. 383 (1965).
[17]N. S. Gillis and N. R. Werthamer, Phys. Rev. 167, 607 (1968).
[18]Such a potential has the effect of drawing the particles together; if one expands the contribution of three-particle correlations to the two-particle equation, the leading term in the expansion will have approximately the same form.
[19]J. A. Krumhansl and S. Y. Wu, Phys. Letters 28A, 263 (1968).
[20]H. Meyer, J. Appl. Phys. 39, 390 (1968).
[21]Because exchange is not included and particles are treated as distinguishable, the statistics of the particles will not actually play any role. We will write equations appropriate for Bose statistics only to simplify the notation.
[22]We use units such that Planck's constant divided by $2\pi$ and Boltzmann's constant are equal to unity.
[23]The notation is generally the same as in L. P. Kadanoff and G. A. Baym, *Quantum Statistical Mechanics* (Benjamin, New York, 1962).
[24]Note that in the frequency component of $G$, $G_{ij}(12, 1'2; \nu)$, the symbols 1, 2, and 1′ represent only the space variables $\vec{r}_1$, $\vec{r}_2$, and $\vec{r}_1'$.
[25]Because the subscripts $\rho$, $\sigma$, and $\alpha$ are all zero starting from this point, we drop them altogether. Also appropriate time ordering is taken here.
[26]L. Fox and E. T. Goodwin, Proc. Cambridge Phil. Soc. 45, 372 (1949).
[27]J. L. Yntema and W. G. Schneider, J. Chem. Phys. 18, 646 (1950).
[28]In the hcp structure, the harmonic expansion is not spherically symmetric beyond the second shell; for more distant shells we use an isotropic approximation as in Ref. 15.
[29]J. S. Dugdale and J. P. Franck, Phil. Trans. Roy. Soc. London A257, 1 (1964).
[30]D. O. Edwards and R. C. Pandorf, Phys. Rev. 140, A816 (1965).
[31]R. C. Pandorf and D. O. Edwards, Phys. Rev. 169, 222 (1968).

PHYSICAL REVIEW A VOLUME 4, NUMBER 1 JULY 1971

# High-Energy Neutron Scattering from Liquid Helium in the Impulse Approximation*

H. A. Gersch and Phil N. Smith
*School of Physics, Georgia Institute of Technology, Atlanta, Georgia* 30332
(Received 19 November 1970)

The impulse approximation is used to describe the inelastic cross section for high-energy neutron scattering from superfluid helium in terms of a ground-state momentum distribution of the helium atoms as given by existing variational calculations. The predicted shape of the cross section is compared with recent experimental data and with a previous theory which approximated the noncondensate contribution to the dynamic structure factor by a single-Gaussian function. In contrast to conclusions obtained using the single-Gaussian approximation, our predicted inelastic cross section omitting a condensate contribution provides an acceptable fit to the experimental data. This fit is worsened by introducing a contribution from a condensate fraction in the amount consistent with the variational calculations, namely 11%. If the condensate fraction is arbitrarily reduced from this value, it is found that a much smaller value, with an upper limit of about 3%, is consistent with the available experimental data. It appears that unique assignments of condensate-fraction contributions to inelastic neutron scattering, for the range of neutron energies presently available, will require an improved theory of final-state effects on the shape of the condensate contribution.

## I. INTRODUCTION

Central to microscopic superfluid theory is the concept of the existence of a condensate fraction of helium particles having zero momentum.[1,2] Recently, experiments in high-energy scattering of neutrons from superfluid helium have been carried out,[3,4] the aim being to measure the momentum distribution of the individual $He^4$ atoms and thus the strength of occupation of the zero-momentum level.[5]

Ideally, one expects a scattering cross section versus energy transfer in the form of a very sharp zero-momentum contribution riding on the top of a much broader background contribution from the noncondensate fraction. Unfortunately, only a single broad peak has been observed in the experiments limited so far to neutron wave-vector transfers of the order of 15 $Å^{-1}$ and to energy resolutions of the order of 4 meV. This circumstance has forced interpretation of the data into considerations of how the over-all shape of the scattering cross section as a function of energy transfer might be modified by a lifetime- and resolution-broadened condensate contribution.[6] Clearly, accurate prediction of condensate-induced shape changes requires a reliable picture of the energy shape of the inelastic cross section without a condensate contribution. Previous analysis[6] has assumed a single-Gaussian energy dependence of the scattering cross section (apart from kinematic factors) for both condensate and noncondensate contributions. That theory has two free parameters: the average kinetic energy per helium particle, which fixes the energy width of the noncondensate contribution to the cross section, and the fraction of particles in the zero-momentum condensate, which fixes the amplitude of the narrower lifetime-broadened condensate contribution. The experimental energy widths were found to be somewhat smaller than that of the theoretical noncondensate contribution, and the required sharpening in energy of the theoretical cross section could be reproduced with a condensate fraction of about 6%.

The work in Ref. 6 is a phenomenological treatment, and as such, provides no detailed relation between the assumed shape of the scattering cross section and the momentum dependence of the individual $He^4$ atoms. To go beyond that phenomenological approach, one would like to solve the central problem of constructing the energy dependence of the cross section from the momentum distribution. In this paper, we do not solve this problem, but rather explore the results obtained from an approximation which does supply a connection between cross section and momentum distribution. This is the impulse approximation, asymptotically valid for high-energy and high-momentum transfer. Physical arguments in support of the validity of the approximation in the relevant experimental region are advanced in Sec. III. Lacking a convincing formal proof of the validity of the impulse approximation, we regard this work as exploring predictions of that approximation, rather than solving the central problem described above.

We make use of existing theoretical predictions of the momentum distribution $n_p$ from variational calculations of the ground-state properties of liquid helium. Unfortunately, corresponding equivalent calculations of $n_p$ at arbitrary temperatures do not seem to be available, so we are restricted in this comparison to temperatures low enough for the ground-state properties to be the dominant factor in the momentum distribution of the helium atoms. We believe this region to encompass at least the lowest temperatures at which neutron experiments have been conducted, namely about 1.2 °K, for reasons enumerated in Sec. III.

Within the impulse approximation, a single-Gaussian energy dependence of cross section also implies a single-Gaussian momentum dependence of $n_p$. Since variational predictions for $n_p$ differ from Gaussian shape, we expect to find a scattering cross section differing from that of Ref. 6. Of course, no conclusions concerning the adequacy of the Gaussian approximation of Ref. 6 can be legitimately drawn from this, because, as already remarked, the phenomenological treatment there given provides no connection between momentum dependence and cross section, and also because the validity of the impulse approximation is not rigorously proved.

We feel there is available sufficient theoretical evidence that $n_p$ for the ground state is not accurately given by a single-Gaussian function of $p$, as it is significantly altered from such a form in two momentum regions. At small-$p$ values, corresponding to the phonon branch of the excitation spectrum in helium, e.g., $p \leq 0.2$ $Å^{-1}$, $n_p$ is expected to vary inversely with $p$, and to be directly proportional to the condensate fraction. This virtual phonon contribution to the ground-state momentum distribution, although it plays a relatively minor role in our results, does have the effect of narrowing the theoretical inelastic scattering cross section for an assumed nonzero value of the condensate fraction, over and above the narrowing produced by the lifetime-broadened condensate itself. A more important effect on theoretical cross-section predictions evolves from the fact that for values of $p$ associated with the roton minimum of the excitation spectrum, $2$ $Å^{-1} \leq p \leq 3$ $Å^{-1}$, $n_p$ is much larger than the Gaussian fit to $n_p$. This effect results in a ground-state distribution in momentum $n_p$ different from a Gaussian (see Figs. 2 and 3) and consequently leads to a predicted inelastic cross section in the absence of a condensate whose dependence on neutron energy transfer is different from the previously assumed Gaussian shape (Figs. 5 and 6). This alteration produces somewhat the same effect as introducing a condensate contribution into the Gaussian analysis as described above, namely a narrowing of the central portion of the inelastic cross section due to scattering from atoms not in the condensate, and also produces an increase in the wing contributions. In this way one gets a creditable fit to the experimental data with-

out a condensate contribution. Adding a condensate contribution from a condensate fraction of 11%, which is the value predicted by ground-state variational calculations, produces a theoretical cross section whose maximum is too high compared with experiment (Fig. 7). This discrepancy is ameliorated by arbitrarily reducing the condensate fraction, and suggests an upper limit of about 3% on the condensate fraction (see Sec. II).

In Sec. II the scattering cross section in the impulse approximation is developed, showing its connection with the momentum distribution $n_p$. Some model predictions of the behavior of $n_p$ for the helium ground state are given, as well as predictions obtained from variational calculations. A fit is made to the variational results, utilizing two Gaussian functions and a modified hyperbola. The dynamic structure factor $S(k, \omega)$ which follows in the impulse approximation from this $n_p$ is compared with that predicted by the single-Gaussian approximation (see Fig. 5), and the inelastic scattering cross sections which follow from these two forms of the structure factor are compared with experimental results (see Figs. 6 and 7).

Section III contains a discussion of the approximations used here, and some possible implications of this work for further experimental investigations.

## II. INELASTIC CROSS SECTION IN THE IMPULSE APPROXIMATION

The inelastic scattering cross section for neutrons on $^4$He liquid is given in the Born approximation by[7]

$$\frac{d^2\sigma}{d\Omega\, d\epsilon_f} = \frac{\sigma_b k_f}{4\pi\hbar k_i}\, S(k, \omega), \tag{1}$$

where $\hbar\vec{k} = \hbar\vec{k}_i - \hbar\vec{k}_f$ is the momentum transferred to the helium, $\hbar\omega = \epsilon_i - \epsilon_f$ is the energy transfer, and $\sigma_b$ is the helium-atom cross section $\sigma_b = 1.13$ b.[6] The dynamic structure factor $S(k, \omega)$ is the Fourier transform of the density-density correlation function

$$S(k, \omega) = (2\pi\rho)^{-1} \int d^3r\, dt\; e^{-i(\vec{k}\cdot\vec{r} - \omega t)} \times [\langle \rho(r, t)\, \rho(0, 0)\rangle - \rho^2] \tag{2}$$

and contains information on the properties of the helium liquid which govern the shape of the inelastic scattering cross section. The average value for the density-density correlation function in Eq. (2) is in general over a canonical ensemble in equilibrium at temperature $T$. We will restrict ourselves to $T = 0$, due to the aforementioned limitation of available theoretical momentum distributions to the ground-state distribution.

In the impulse approximation the interactions between helium atoms (during the neutron-helium interaction time) are neglected; the neutron can be pictured as striking a helium atom between collisions of the helium atom with other helium atoms. This simple-minded picture allows us to find the form of $S(k, \omega)$ in the impulse approximation. Conservation of energy and momentum in the neutron-helium collision gives the relation between energy loss and momentum transfer:

$$\hbar\omega = (\hbar^2k^2/2m) + (\hbar\vec{k}\cdot\vec{p}/m), \tag{3}$$

where $m$ is the helium atom and $\vec{p}$ is its momentum before collision. One sees that the neutron energy loss $\hbar\omega$ depends on the distribution of helium momentum $\vec{p}$ parallel to the neutron momentum transfer $\hbar\vec{k}$. Atoms in the condensate have $p = 0$ and give rise to neutrons having suffered the unique energy loss

$$\hbar\omega_0 = \hbar^2k^2/2m\ . \tag{4}$$

Helium atoms with nonzero momentum in a direction parallel to the neutron momentum transfer provide a spread in neutron energy loss symmetrically distributed about $\hbar\omega_0$. Since there will be no scattering unless the conditions of Eq. (3) are satisfied, we expect $S(k, \omega)$ to be given by a $\delta$ function with argument $\hbar\omega - \hbar^2k^2/2m - \hbar\vec{k}\cdot\vec{p}/m$, multiplied by $n_p$, the number of atoms having momentum $p$, and then summed over all $p$:

$$N\, S(k, \omega) = \sum_{\vec{p}} n_p \delta(\omega - k^2/2m - \vec{k}\cdot\vec{p}/m) \tag{5}$$

(we put $\hbar = 1$ in this and subsequent relations). Equation (5) is correct for $k \to \infty$ in the impulse approximation, as is easily verified by calculating the density-density correlation function for a free-particle system. However, we assume, in accordance with our previous remarks, that $n_p$ in Eq. (5) is the momentum distribution of the individual interacting helium atoms in the ground state. Thus, we take the struck helium atom to respond to the neutron as a free particle, with the effect of helium-helium interactions as providing an initial momentum distribution peculiar to the ground state. Our crucial assumption is that of extrapolating the region of validity of the impulse approximation from $k \to \infty$, in which limit the incoming neutron cannot distinguish between condensate and noncondensate $He^4$ atoms at all, to the range of experimental $k$ values used in Ref. 4. This assumption is discussed in Sec. III.

Replacing the sum in Eq. (5) by an integral, and integrating over the angle between neutron momentum transfer $\vec{k}$ and helium-atom momentum $\vec{p}$ one gets

$$S(k, \omega) = S_0(k, \omega) + S_1(k, \omega), \tag{6}$$

where $S_0(k, \omega)$ is the condensate contribution, omitting lifetime effects for the time being:

$$S_0(k, \omega) = n_0\, \delta(\omega - \omega_0). \tag{7}$$

Here $n_0 = N_0/N$ is the condensate fraction. The non-

condensate contribution $S_1(k, \omega)$ is given by

$$S_1(k, \omega) = (m/4\pi^2 k\rho)\int_{p_{\min}}^{\infty} p\, n_p dp. \quad (8)$$

Here $p_{\min}$ is the magnitude of the smallest helium momentum parallel to $\vec{k}$ which will give the neutron the energy loss $\omega$:

$$p_{\min} = \frac{|\omega - \omega_0|}{k/m} . \quad (9)$$

For fixed momentum transfer $k$, this minimum momentum increases linearly with the deviation of the energy loss $\omega$ from the value $\omega_0 = k^2/2m$. Thus, for $\omega = \omega_0$, all the helium atoms with nonzero momenta contribute to $S_1(k, \omega)$. As the neutron energy loss $\omega$ departs from $\omega_0$, the lowest-momentum helium atoms no longer participate in the scattering, and as the energy loss departs significantly from the value $\omega_0$ only the higher-momentum helium atoms make a contribution to the scattering. As Eq. (8) indicates, the slope of $S_1(k, \omega)$ as a function of $\omega$ for $k$ fixed measures the product $p\, n_p$ evaluated at $p_{\min}$:

$$\left| \frac{\partial S_1(k, \omega)}{\partial \omega} \right| = \frac{m^2}{4\pi^2 k^2 \rho} (p\, n_p)\, p_{\min} . \quad (10)$$

Equation (10) provides confirmation of our previous remark that a Gaussian $\omega$ dependence of $S_1(k, \omega)$ implies a Gaussian dependence of $n_p$ on $p$: If $S_1(k, \omega) \sim e^{-\alpha(\omega-\omega_0)^2}$, then $n_p \sim e^{-\alpha p^2}$, with $\alpha = am^2/k^2$. This form may represent a reasonable dependence of $n_p$ on $p$ at temperature considerably above the $\lambda$ temperature. However, in the ground state, $n_p$ should reflect the general characteristic peculiar to boson ground states, namely, that of containing zero-point oscillations of the excitations. In the small-$p$ region one expects a significant contribution to $n_p$ from zero-point oscillations of the low-lying phonon modes. In the region around the roton minimum in the excitation spectrum, one may again expect a contribution to $n_p$ from the zero-point oscillations of these relatively low-lying modes. Admittedly, this argument has no rigorous foundation when applied to real helium. The distribution $n_p$ measures the strength of the poles of the one-particle Green's function $G_1(p, \omega)$, while the excitation spectrum $\mathcal{E}(p)$ determined by inelastic neutron scattering locates the $\delta$-function peaks of $S(p, \omega)$, related to the poles of the two-particle Green's function. For the low-momentum limit, there are arguments that the spectrum of density fluctuations should correspond to the spectrum of single-particle excitations.[8] However, there is no *a priori* reason why this correspondence should extend to the higher-momentum roton region, so that the argument given above can have only a suggestive character applied to real helium. This suggestive character is replaced by a precise connection between $n_p$ and $\mathcal{E}(p)$ in two model theories for which the poles of the one- and two-particle Green's functions do coincide. One of these is the Bogolyubov theory of a dilute superfluid system, for which[9]

$$n_p = \frac{(mc^2)^2}{2\mathcal{E}(p)\,[\mathcal{E}(p) + p^2/2m + mc^2]} . \quad (11)$$

Here $c$ is the speed of sound in the dilute system. In the phonon region, $\mathcal{E}(p)$ varies linearly with $p$, and Eq. (11) predicts the dependence $n_p \sim 1/p$. The elementary spectrum $\mathcal{E}(p)$ of Bogolyubov does not produce the roton minimum. We attempt to correct that deficiency by using in Eq. (11) the experimental $\mathcal{E}(p)$ curve obtained from neutron scattering[10] and the value of $c$ appropriate to liquid He. This yields an $n_p$ vs $p$ as shown in Fig. 1, exhibiting a roton bump in $n_p$ for values of $p$ around 2 Å$^{-1}$. Of course, inserting the correct $\mathcal{E}(p)$ in a theoretical approximation which itself is incapable of producing it is questionable. However, since the low-density superfluid theory has proven quite useful in a qualitative way when scaled to actual helium density, we expect some validity to the qualitative result that there are more atoms in the ground state with momenta around 2 Å$^{-1}$ than would be given by a single Gaussian in $p$, centered at $p = 0$.

Another explicit connection between $n_p$ and $\mathcal{E}(p)$ is provided by a cell model of the superfluid ground state which is not limited to low density.[11] This model, which predicts a condensate fraction of at least 6% for ground-state helium yields an $n_p$-vs-$p$ curve with the same qualitative behavior as that obtained from Bogolyubov theory, with a somewhat more pronounced roton bump.

These model theory results are presented simply to give some additional supporting evidence for the characteristics of $n_p$ as found from variational calculations of ground-state properties of liquid helium.[12–14] These latter calculations all yield a very similar dependence of $n_p$ on $p$, except in the phonon region, where only Ref. 14 produces the $1/p$ dependence for low-$p$ values. In Fig. 2 we give the result for $n_p$ vs $p$ as found in Ref. 12. We will shortly modify the low-momentum dependence shown in the figure to bring it into agreement with the results of Ref. 14. The roton bump of the model theories is clearly in evidence in the region $2 \leq p \leq 3$ Å$^{-1}$ of Fig. 2, although the variational calculations have subdued the bump into something more like a shoulder. This shoulder may appear to be a rather small contribution to the total momentum distribution, but atoms in this region, estimated to be about 15% of the total number, carry a much larger fraction, about 45% of the total ground-state kinetic energy.[12] (See Fig. 3, in which $p^2 n_p$ is plotted versus $p$.)

Suppose, following the approach in Ref. 6, we try to fit the dynamic structure factor $S_1(k, \omega)$ with a single Gaussian centered on $\omega_0$. Then in the impulse approximation, this is equivalent to fitting $n_p$

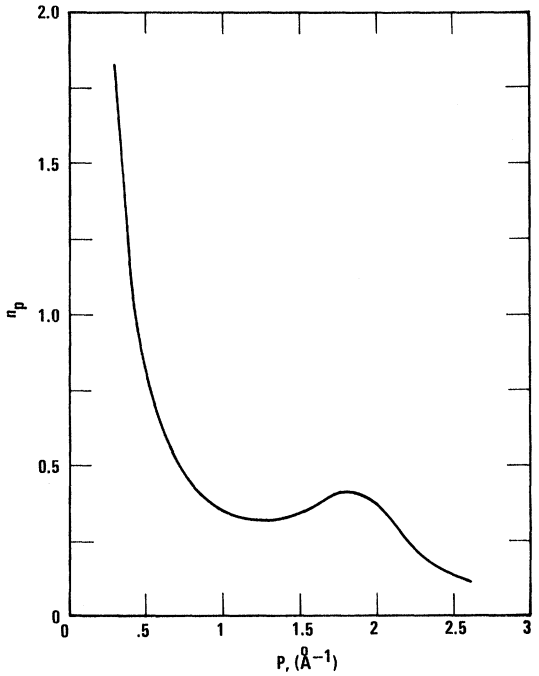


FIG. 1. Ground-state momentum distribution function $n_p$ for liquid $He^4$ as given by Bogolyubov theory, utilizing experimental excitation energies $\mathcal{E}(p)$ in Eq. (11).

with a single Gaussian centered on zero momentum and having the same kinetic energy per helium atom as given by the variational calculations, about 14.16 °K. Clearly, such a Gaussian will not contain the requisite number of atoms near $p \sim 2.5$ Å$^{-1}$, and so will have to be broader than the variational results in order to produce the required kinetic energy. In Fig. 3 we have compared the quantity $p^2 n_p$ for such a Gaussian,

$$n_p = 0.451\, e^{-0.642\, p^2}, \tag{12}$$

with the corresponding quantity from the variational calculations. The comparison shows clearly that Eq. (12) overestimates the number of atoms in the region from about 1 to 2 Å$^{-1}$, as well as underestimating the occupation for those atoms with momentum about 2.5 Å$^{-1}$.

We have found it possible to get a good fit to McMillian's data, modified to give the $1/p$ dependence at small-$p$ values, with the following functional form for $n_p$:

$$n_p = (p_0/p)\, e^{-(p/p_c)^2} + A\, e^{-ap^2} + B\, e^{-b(p-p_s)^2}. \tag{13}$$

The first term in Eq. (13) represents mainly the contribution to the single-particle momentum coming from the zero-point phonon oscillations. The exponential factor in this term serves to cut off this contribution as $p$ increases above $p_c$. The second term is designed to reproduce the nonphonon part of the momentum distribution out to values of $p$

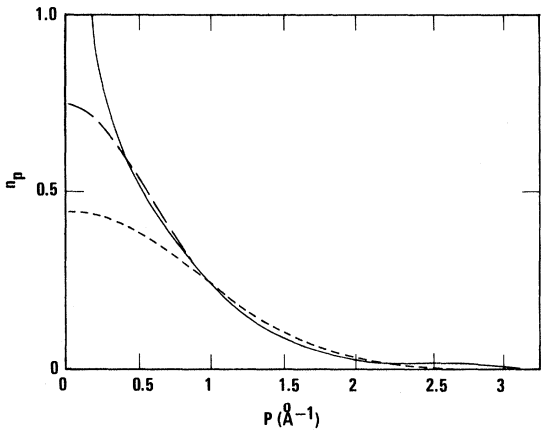


FIG. 2. Ground-state momentum distribution function $n_p$ for liquid $He^4$, as given by Ref. 12 (long-dashed line); empirical fit, as given by Eq. (13) (solid line); and single-Gaussian fit, Eq. (12) (short-dashed line).

near 1.5 Å$^{-1}$. The third term reproduces the roton bump.

The momentum $p_0$, which determines the strength of the phonon contribution to $n_p$, is given both by perturbation theory[8] and by variational calculations[14] as

$$p_0 = n_0^{\frac{1}{2}} mc, \tag{14}$$

where, as before, $c$ stands for the speed of sound in helium, and $n_0$ the condensate fraction. The corresponding dilute superfluid theory result which follows from Eq. (11) corresponds to $p_0 = \frac{1}{2}mc$, consistent with its fundamental assumption of negligible depletion, i.e., $n_0 = 1$. Note that the condensate fraction $n_0$ enters the scattering cross-section formula in both the unique condensate contribution expressed by $S_0(k, \omega)$ of Eq. (7) and the enhanced low-momentum occupation $n_p$, which contributes to the noncondensate contribution $S_1(k, \omega)$ of Eq. (8).

The numerical values of $p_0$ and the other empirical constants were determined in the following manner. In order to minimize theoretical inconsisten-

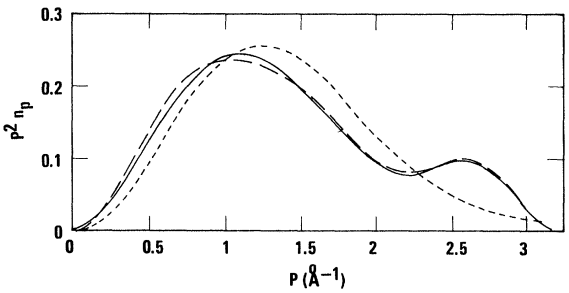


FIG. 3. Quantity $p^2 n_p$ for ground-state $He^4$: long-dashed line, as given by Ref. 12; short-dashed line, from the single-Gaussian fit, Eq. (12); and solid line, from the empirical fit, Eq. (13).

cies, we used the same condensate fraction $n_0 = 0.11$ and sound speed $c = 267$ m/sec as those calculated by McMillan.[12] For these choices, $p_0 = 0.0929$ Å$^{-1}$.

The remaining parameters were determined by trial. In Ref. 12 plots of the nonphonon contributions to both $n_p$ and $p^2 n_p$ are presented. The second of these shows more structure than the first and thereby serves to establish more precisely the values of fitting parameters. We consequently tabulated $p^2 n_p$ and then varied parameters to get a least-squares fit. The variation was performed in two stages. First, the roton-shoulder term was omitted from Eq. (13); and the parameters $p_c$, $A$, and $a$ were varied independently until we obtained a best fit to twelve points equally spaced over the momentum interval $0.7 \le p \le 1.8$ Å$^{-1}$. By this procedure we found $p_c = 0.77$ Å$^{-1}$, $A = 0.4832$, and $a = 0.772$ Å$^2$. Next, these values were substituted into Eq. (13); and the parameters $B$, $b$, and $p_s$ were varied independently. A best fit to seven points equally spaced over the region $2.3 \le p \le 2.9$ Å$^{-1}$ was attained for $B = 0.0118$, $b = 7.45$ Å$^2$, and $p = 2.57$ Å$^{-1}$. Figure 4 shows the quantity $pn_p$ as a function of ground-state momentum $p$, both as determined by the single-Gaussian fit, Eq. (12), and by the fit to the variational calculations, Eq. (13). As we have seen earlier in Eq. (8), the quantity $pn_p$ determines the $\omega$ dependence of $S_1(k, \omega)$ and hence the energy dependence of the inelastic cross section. In addition to those differences already noted in conjunction with the discussion of Fig. 3, we see from Fig. 4 that the zero-point phonon contribution to $n_p$ makes the variational-based $pn_p$ nonzero at $p = 0$. Equation (10) then predicts a finite nonzero slope for $S_1(k, \omega)$ at $\omega = \omega_0$, contrasted with the zero slope predicted by the single-Gaussian approximation.

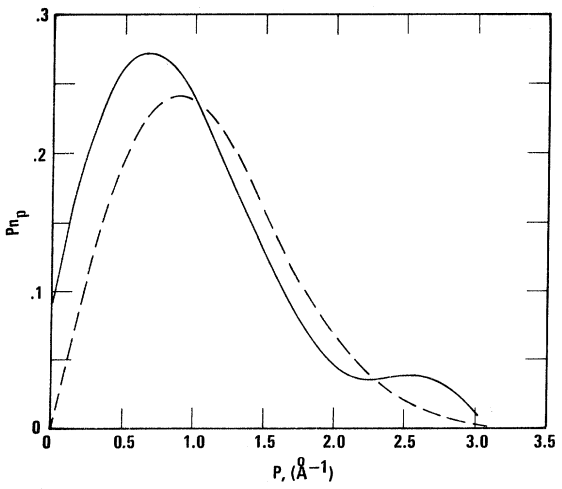


FIG. 4. Quantity $pn_p$ for ground-state helium: solid line, from empirical fit, Eq. (13); dashed line, from single Gaussian, Eq. (12).

Thus the zero-point phonon contributions provide a further sharpening in the shape of $S_1(k, \omega)$ and hence of the inelastic cross section.

The noncondensate contribution to the dynamic structure factor $S_1(k, \omega)$ can be written utilizing Eqs. (8) and (13) in the closed form:

$$S_1(k,\omega) = \frac{m}{4\pi^2 k\rho}\left[p_0 p_c \operatorname{erfc}\left(\frac{p_{\min}}{p_c}\right) + \frac{A}{2a} e^{-a p_{\min}^2} + \frac{B}{2b} e^{-b(p_{\min}-p_s)^2} + \frac{B p_s}{2}\left(\frac{\pi}{b}\right)^{1/2} E(p_{\min}, p_s)\right]. \quad (15)$$

Here

$$\operatorname{erfc}(x) = 1 - \operatorname{erf}(x) = 2\pi^{-1/2}\int_x^\infty e^{-t^2} dt, \quad (16)$$

$$E(p_{\min}, p_s) = \begin{cases} 2 - \operatorname{erfc}(b^{1/2}|p_{\min} - p_s|), & p_{\min} < p_s \\ \operatorname{erfc}(b^{1/2}(p_{\min} - p_s)), & p_{\min} > p_s \end{cases}. \quad (17)$$

To get the total dynamic structure factor, we must add to $S_1(k, \omega)$ the condensate contribution $S_0(k, \omega)$. We will consider this contribution in two forms. One form is the ideal $\delta$ function of Eq. (7), applicable for very short neutron-helium interaction times so that He-He collisions play no role in the scattering. The other form, which attempts to account for the effect of the He-He collisions, is a phenomenological lifetime-broadened $S_0(k, \omega)$ introduced in Ref. 5 and adopted in Ref. 6 in the form of a Gaussian shape:

$$S_0(k,\omega) = n_0\left(\frac{\pi}{\gamma_1(k)}\right)^{1/2} e^{-\gamma_1^{-1}(\omega-\omega_0)^2}. \quad (18)$$

Here $\gamma_1^{-1/2}$ is a measure of the lifetime of atoms in the condensate:

$$\gamma_1 = \frac{1}{4\ln 2}\,\Gamma_1^2, \quad (19)$$

where $\Gamma_1$, the full width at half-maximum of the condensate peak, is taken to be[6]

$$\Gamma_1 = \rho\sigma k/m. \quad (20)$$

In Refs. 5 and 6 the He-He scattering cross section $\sigma$ was taken as $2\times10^{-15}$ cm$^2$. However, both theory and experiment seem to indicate a larger value, $\sigma = 4\times10^{-15}$ cm$^2$,[15] and we choose this latter estimate. Equation (18) is discussed further in Sec. III.

Combining Eq. (15) and either of Eq. (7) or (18). yields the complete dynamic structure factor. The structure factor is plotted in Fig. 5 as a function of the variable $p_{\min} = |\omega - \omega_0|/(k/m)$ of Eq. (9) and for fixed momentum transfer $k$. The solid curve of Fig. 5 is obtained utilizing the lifetime-broadened $S_0$ of Eq. (18), with a condensate fraction equal to 0.11. The line of long dashes in the figure

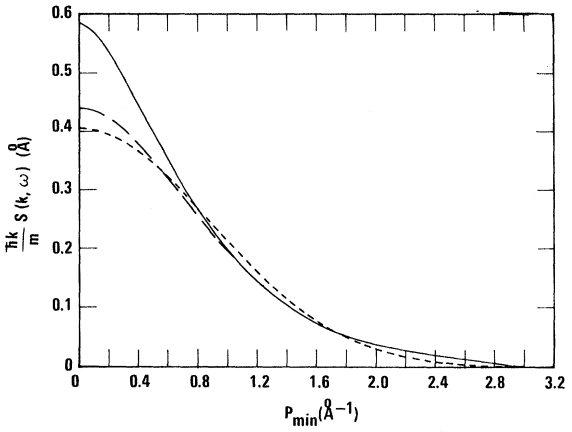


FIG. 5. Theoretical dynamic structure factor $S(k, \omega)$ for ground-state helium vs variable $p_{\min}$ given by Eq. (9) for fixed momentum transfer $k$. Solid line is obtained using lifetime-broadened $S_0(k, \omega)$, Eq. (18), and a condensate fraction $n_0 = 0.11$. Long-dashed line corresponds to $S(k, \omega)$ with condensate fraction contribution omitted. Short-dashed line is the single-Gaussian approximation, $n_0 = 0$.

is $S(k, \omega)$, omitting a contribution from the condensate fraction. Since $n_0 = 0$, Eq. (13) is inapplicable here; this line represents the result of numerical integration, according to Eq. (8), of a tabulation of McMillan's $n_p$.

The single-Gaussian $n_p$ of Eq. (12), corresponding to $n_0 = 0$, produces an $S(k, \omega)$ shown in Fig. 5 as the line of short dashes. We have chosen to normalize the two curves in Fig. 5 corresponding to $n_0 = 0$ to an area of 0.89, while the solid curve for $n_0 = 0.11$ is normalized to unit area, so that the lifetime-broadened condensate contribution to $S(k, \omega)$ is given by the difference between the solid and dashed curves in Fig. 5. As previously remarked, the condensate makes a contribution to $S(k, \omega)$ both through $S_0(k, \omega)$ and also through the zero-point phonon contribution to $S_1(k, \omega)$. In Fig. 5, at the peak of $S(k, \omega)$, about one-third of the difference between the solid ($n_0 = 0.11$) and dashed ($n_0 = 0$) curves comes from the zero-point phonon contribution and two-thirds of the difference is due to $S_0(k, \omega)$. These particular fractional contributions to the sharpening of the structure factor depend, of course, on the amount of lifetime broadening assumed for $S_0(k, \omega)$. For a sharper $S_0(k, \omega)$, the zero-point phonon contribution to the peak of $S(k, \omega)$ would be fractionally smaller.

Comparing the two $n_0 = 0$ curves of Fig. 5, we see, as expected, that the single Gaussian is a somewhat broader function of $p_{\min}$ than its counterpart from the variational calculations, and lacks the wing contributions given by the latter.

Finally, we compare our results with the experimental measurements of Harling[4,16] for neutrons of initial energy 0.1715 eV, scattered off liquid helium at 1.265 °K, with a fixed scattering angle of 154.3°. The experimentally determined cross section as a function of neutron energy loss is depicted in Fig. 6. Using the single-Gaussian theory, Puff and Tenn in Ref. 6 found a best fit to these data for a condensate fraction $n_0 = 0.06$. We now wish to see how this result compares with the predictions following from our fit to the variational calculations for $n_p$. To this end we utilize Eqs. (1) and (15) and either of Eq. (7) or (18).

Experimental resolution broadening is accounted for by convoluting the theoretical cross section given by Eq. (1) with the experimental resolution function $R(\omega - \omega')$[16]:

$$R(\omega - \omega') = (\pi\Gamma_R)^{-1/2} \exp[-\Gamma_R^{-1/2}(\omega - \omega')^2], \quad (21)$$

where $\Gamma_R$ is given in terms of the instrumental resolution $\Delta E = 3.4$ meV as

$$\Gamma_R = (\Delta E)^2/4\ln 2. \quad (22)$$

To account for the experimental arrangement of fixed scattering angle, rather than fixed momentum transfer $k$, we use the kinematic relation giving $k$ as a function of energy loss $\omega$ for fixed angle $\theta$ and incident energy $\epsilon_i$:

$$k^2 = \tfrac{1}{2}m\{2\epsilon_i[1 - \cos\theta\,(1 - \omega/\epsilon_i)^{1/2}] - \omega\}. \quad (23)$$

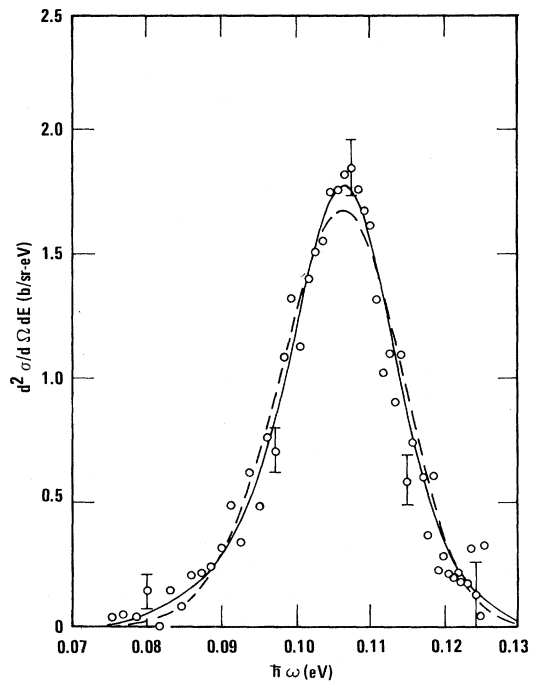


FIG. 6. Inelastic cross section for neutrons on $He^4$ liquid vs energy transfer $\hbar\omega$. Circles are the experimental data from Refs. 4 and 16, with the vertical bars indicating statistical accuracy. Single-Gaussian theory ($n_0 = 0$) produces the dashed curve, and solid line is present calculation with the condensate omitted.

With these adjustments, we plot theoretical values for the absolute cross section with no condensate contribution in Fig. 6. The dashed line is the prediction of the single-Gaussian theory. This curve has a maximum which falls somewhat below the experimental peak, is a little too broad, and gives insufficient wing contributions to the scattering. It was precisely these deficiencies which could be improved upon in Ref. 6 by the addition of a narrower condensate contribution.

For comparison, the solid curve in Fig. 6 represents the inelastic cross-section prediction of the present theory with the condensate omitted, which removes both the condensate contribution to $S_0(k, \omega)$ and also the zero-point phonon contribution to $S_1(k, \omega)$. One sees from the figure that the above-mentioned deficiencies of the single-Gaussian approximation compared with experiment are no longer present, the experimental data being quite well represented by the solid curve.

To see if the experimental data will support a condensate contribution, we also show in Fig. 7 the scattering cross section assuming a condensate fraction $n_0 = 0.11$. The dashed curve of Fig. 7 utilizes the $\delta$ function $S_0(k, \omega)$, so that the condensate contribution has the shape of the experimental resolution function, Eq. (21). The solid curve in Fig. 7 depicts the lifetime-broadened condensate contribution for $S_0$ given by Eq. (18). The smaller value for the He-He scattering cross section adopted in Refs. 5 and 6 would yield a scattering cross-section shape near the peak intermediate between these two shown in Fig. 7. In any event, it is clear that the comparison with experiment is worsened by introducing a condensate fraction contribution corresponding to $n_0 = 0.11$. The zero-point phonon contribution to $S_1(k, \omega)$ represented by the first term in Eq. (13) plays a relatively minor role in sharpening the cross section peak. We calculate its contribution to the cross section at the peak to be about one-third of that contributed by $S_0(k, \omega)$.

Arbitrarily reducing the condensate fraction from the value $n_0 = 0.11$ used to obtain the curves of Fig. 7 will of course reduce the discrepancy between theory and experiment. It is clear from the figure that a drastic reduction in $n_0$ is required to bring the dashed curve, which omits lifetime effects, into agreement with experiment. The resulting value for $n_0$ is far too small to be significant. On the other hand, the lifetime-broadened curve, shown as a solid line in Fig. 7, requires a much smaller reduction in $n_0$. We estimate that the experimental data are consistent with a lifetime-broadened contribution from a condensate fraction of 0.03. Considering that the broadening of $S_0(k, \omega)$ due to final-state interactions is probably overestimated by the solid curve (see Sec. III), even this small value of $n_0$ must be regarded as an upper limit, so that its significance is questionable.

## III. DISCUSSION

Central to our analysis is the impulse approximation which has provided a direct connection between the momentum distribution of the atoms in the ground state of superfluid helium and the inelastic neutron scattering cross section. Therefore, some indication of its validity under the experimental conditions we have analyzed seems to be in order. This is especially true since there is both theoretical and experimental evidence of the inadequacy of the impulse approximation for neutrons scattered with smaller momentum transfers than the value of about 14.3 $\text{Å}^{-1}$ used by Harling, say $k$ from 2 to about 9 $\text{Å}^{-1}$.[3,17,18] For this region of momentum transfer the peak of the inelastic scattering cross section was observed to occur at values of $\omega$ different from the free-particle value $\omega_0 = \hbar^2k^2/2m$, and the widths of the scattering peaks were found to oscillate about the simple linear in $k$ dependence, which is expected for scattering in the impulse approximation.[3] This behavior has been explained by introducing the effect of helium-helium interactions as an effective $k$-dependent interaction $\Sigma(k)$ modifying the free-particle behavior, so the single-particle energy becomes $\mathcal{E}(k) = \hbar^2k^2/2m + \Sigma(k)$.[17] The

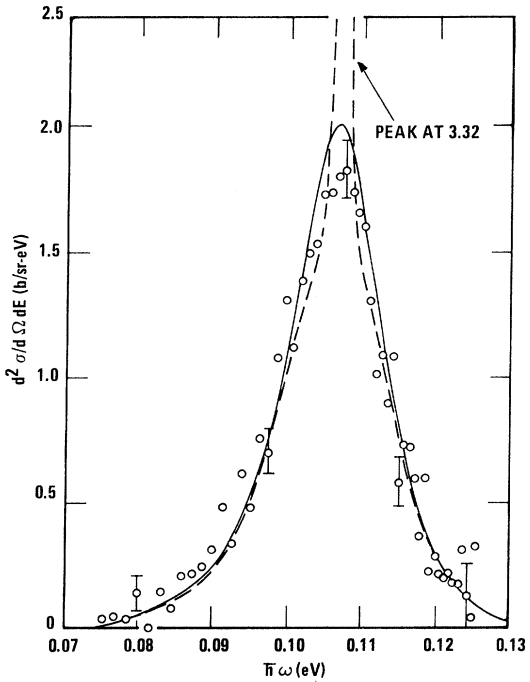


FIG. 7. Effect of including a condensate contribution to the inelastic neutron cross section for scattering off liquid helium. Dashed curve includes an $S_0(k, \omega)$ given by the $\delta$ function of Eq. (7). Solid curve is for lifetime-broadened $S_0(k, \omega)$ given by Eq. (18). Condensate fraction is $n_0 = 0.11$.

form for $\Sigma(k)$ found, utilizing the $f$-sum rule, was $\Sigma(k) = (a\hbar^2/2m)\cos kr_0$, with $a \simeq 2.5$ Å$^{-2}$ and $r_0$ the hard-core diameter. Now for the momentum transfers in Harling's experiment where $k \approx 14.3$ Å$^{-1}$, this effective interaction $\Sigma$ is only about 1% of the free-particle energy, which is experimentally undetectable. This prediction is consistent with the experimental result that no detectable deviation in the location of the scattering peak from the free-particle value $\omega = \omega_0$ was found for the range of $k$ values above about 10 Å$^{-1}$.[6,16] These results support the validity of neglecting He-He collisions in determining the shape of the scattering cross section from helium atoms not in the condensate. The same conclusion follows from a crude calculation which compares the neutron-helium collision time $t_n$ with the He-He collision time $t_h$. The validity of the impulse approximation requires $t_n \ll t_h$, so that a neutron can be pictured as striking a helium atom between helium-helium collisions. We use the uncertainty principle to estimate $t_n \approx \hbar/\Delta E \approx 2m/\hbar k^2$, while for $t_h$ we may use our previous estimate of lifetime for the condensate, $t_h = m/\hbar k \rho\sigma$. Therefore the free-particle scattering conditions require

$$2m/\hbar^2 k^2 \ll m/\hbar k \rho\sigma$$

or

$$1/k \ll 0.63 \text{ Å} .$$

For Harling's experiment, where $k = 14.3$ Å$^{-1}$, this inequality seems to be well satisfied, so that He-He collisions should play a minor role in distorting $S_1(k, \omega)$ from its impulse-approximation shape. Of course, these collisions are expected to have a more important effect in broadening the $\delta$-function shape of $S_0(k, \omega)$. The phenomenological lifetime-broadened $S_0$ given in Eq. (8) is probably an overassessment of the effect of He-He collisions, since according to our estimate of times involved, the neutron-helium collision time is considerably shorter than the helium lifetime due to collisions with other helium atoms. This argument leads us to suspect that a better theory of the shape of $S_0(k, \omega)$ would only increase the discrepancy between experiment and the theoretical cross section shown as the solid curve in Fig. 7.

Another crucial assumption we have employed is that one can utilize the ground-state momentum distribution $n_p$ to describe liquid helium at a temperature of 1.265 °K. One might argue that the distinguishing features of the ground state $n_p$, namely the roton bump at $p \simeq 2.5$ Å$^{-1}$ and the phonon enhancement at small $p$, will get washed out with temperature, producing at 1.265 °K an $n_p$ curve very much like the single Gaussian depicted in Fig. 3. We think this is unlikely. First of all, the mean thermal energy at 1.265 °K is only a small fraction of the average ground-state kinetic energy of 14.2 °K, so in a crude way, only a very small readjustment in number distribution should take place near the roton bump, where the atoms carry kinetic energy considerably larger than the mean value. The wing contributions to $S(k, \omega)$ which are present in Harling's experiment can be taken as evidence that the roton-bump contribution persists to at least this temperature of 1.265 °K. However, this roton bump in $n_p$ should disappear at the highest temperatures at which neutron scatterings have been measured, namely about 4.2 °K, at which temperature the helium atoms are expected to be well approximated by a free-particle Gaussian distribution.[19] According to our previous analysis, this implies (see Fig. 3) a contribution to the broadening of the main neutron scattering peak between 1.2 and 4.2 °K independent of any broadening due to a disappearing condensate. Therefore, experimental evidence of such increase in energy width with temperature does not constitute unambiguous evidence for a vanishing condensate distribution.

The small-$p$ behavior of $n_p$ is, by contrast, expected to change more rapidly with temperature: $n_p \sim kT/p^2$ for $T$ finite, rather than $n_p \sim 1/p$ for $T = 0$.[14] However, this altered behavior of $n_p$ occurs only at very-small-$p$ values, $p \lesssim 0.1$ Å$^{-1}$ at $T \approx 1$ °K. The contribution to $S(k, \omega)$ from this small-$p$ region is completely inside of experimental resolutions. The sharpening of the resolution-broadened scattering cross section due to this changed low-$p$ behavior appears to be completely negligible at $T = 1.2$ °K.

It seems clear that experiments to find a unique contribution to the scattering cross section from the condensate should concentrate attention near the scattering peak, and aim to reduce statistical uncertainty in count rates. It would probably be worthwhile to do the experiments at lower temperatures, to test the adequacy of utilizing the ground-state momentum distribution to predict cross-section shapes. Reliable measurements of the temperature dependence of the wing contributions to the scattering cross section, which in the impulse approximation come from the helium atoms in the roton bump, would provide a useful test of the adequacy of this approximation.

It would also, of course, be desirable to use neutrons of higher initial energy, say 1 eV, in order for final-state effects on the condensate scattering contribution to be negligible. However, this does not presently appear feasible with reactor neutrons.

Our estimate for the condensate fraction $n_0 \lesssim 0.03$ seems uncomfortably small compared with theoretical predictions for this quantity. A sufficiently strong bias in favor of a larger $n_0$, e.g., between about 0.05 and 0.10, might lead one to infer that our results argue for a better relation between $S(k, \omega)$ and momentum distribution $n_p$ than that provided by the impulse approximation. The situation clearly calls for a more rigorous justification of

the impulse approximation.

ACKNOWLEDGMENTS

The authors wish to express their thanks to Dr. O. K. Harling for making available his experimental results and for communications and discussions concerning this work.

*Work supported by NSF Grant No. GP 14058.

[1]F. London, *Superfluids* (Wiley, New York, 1954), Vol. II.

[2]O. Penrose and L. Onsager, Phys. Rev. 104, 576 (1956).

[3]R. A. Cowley and A. D. B. Woods, Phys. Rev. Letters 21, 767 (1968).

[4]O. K. Harling, Phys. Rev. Letters 24, 1046 (1970).

[5]Such experiments were suggested by P. C. Hohenberg and P. M. Platzman, Phys. Rev. 152, 198 (1966).

[6]R. D. Puff and J. S. Tenn, Phys. Rev. A 1, 125 (1970).

[7]L. Van Hove, Phys. Rev. 95, 249 (1954).

[8]J. Gavoret and P. Nozières, Ann. Phys. (N. Y.) 28, 349 (1964).

[9]See, e.g., A. A. Abrikosov, L. P. Gorkov, and I. E. Dzyaloshinski, *Methods of Quantum Field Theory in Statistical Physics* (Prentice-Hall, Englewood Cliffs, N. J., 1963), Chap. 1.

[10]D. G. Henshaw and A. D. B. Woods, Phys. Rev. 121, 1266 (1961).

[11]H. A. Gersch and J. M. Tanner, Phys. Rev. 139, 1769 (1965). Equations (81) and (110) of this paper provide the connection between $n_p$ and $\mathcal{E}(p)$.

[12]W. L. McMillan, Phys. Rev. 138, A442 (1965).

[13]D. Schiff and L. Verlet, Phys. Rev. 160, 208 (1967).

[14]W. P. Francis, G. V. Chester, and L. Reatto, Phys. Rev. A 1, 86 (1970).

[15]R. B. Bernstein and F. A. Morse, J. Chem. Phys. 40, 917 (1964).

[16]O. K. Harling (private communication).

[17]J. F. Fernandez and H. A. Gersch, Phys. Letters 30A, 261 (1969).

[18]V. F. Sears, Phys. Rev. 185, 200 (1969).

[19]In support of this expectation, the wing contributions to the scattering peak, due to atoms with momentum near the roton bump and clearly present at 1.2 °K, seem to have disappeared at 4.3 °K. The situation is not as clear as one would like, owing to poor statistics and uncertain background subtractions.

PHYSICAL REVIEW A VOLUME 4, NUMBER 1 JULY 1971

# Polarization Effects in Zeeman Lasers with $x$-$y$-Type Loss Anisotropies

Albert Le Floch and Roger Le Naour
*Laboratoire d'Electronique Quantique, Faculté des Sciences, Avenue du Général Leclerc, Rennes, Ille et Vilaine, France*

(Received 12 June 1970; revised manuscript received 29 October 1970)

It has already been reported that a laser subject to an axial magnetic field and having end mirrors which exhibit relatively high $x$-$y$-type loss anisotropy can be described by two theoretical methods. The first method uses self-consistent-field equations with distributed losses, whereas the second one is based on a resonance condition for a complete round-trip pass. The following study of a Zeeman laser with different $x$-$y$-type loss anisotropy at each mirror shows that the localization of the losses and the nonreciprocal character of the Farady rotation require a different formulation for each initial system. The rotation of the plane of polarization is different at each end of the laser, but it is shown that there always exists for central tuning a real or virtual average polarization vector which obeys Lamb's theory. The equivalence of the two methods is discussed.

## I. INTRODUCTION

Lamb's self-consistent theory, which supposes distributed losses within the laser cavity, has been shown to be correct when extended to treat the electric field polarization properties of lasers with isotropic or weakly anisotropic cavities.[1-3]

In a recent paper, Greenstein[4] stated the difficulties of the self-consistent-field method, and compared the results with those given by a resonance condition for a complete round-trip pass[5] in a single centrally tuned laser, for a particular cavity where all $x$-$y$ anisotropic losses were localized at one mirror. It was seen that, in general, the two sets of results did not agree except in the limit of small anisotropy. Consequently, Greenstein concluded that the two methods are not equivalent and only the resonance condition gives a correct description of the polarization for large cavity anisotropy. In particular, he points out that the maximum amount of rotation of the plane of polarization is always somewhere between $\frac{1}{4}\pi$ and $\frac{1}{2}\pi$, and approaches 90° in the limit of strong anisotropy ($\epsilon \to 1$); this result is inconsistent with that given by the self-consistent method, which however predicts much more in the limit of small anisotropy.

The following paper discusses the general case of a cavity with an anisotropic $x$-$y$ mirror at each